

Outgoing electromagnetic power induced from pair plasma falling into a rotating black hole

Yasufumi Kojima [★]

Department of Physics, Hiroshima University, Higashi-Hiroshima, 739-8526, Japan

27 March 2021

ABSTRACT

We examine energy conversion from accreting pair plasma to outgoing Poynting flux by black hole rotation. Our approach is based on a two-fluid model consisting of collisionless pair plasma. The electric potential is not constant along magnetic field lines, unlike an ideal magnetohydrodynamics approximation. We show how and where longitudinal electric fields and toroidal magnetic fields are generated by the rotation, whereas they vanish everywhere for radial flow in a split monopole magnetic field in a Schwarzschild black hole. Outgoing electromagnetic power in a steady state is calculated by applying the WKB method to the perturbation equations for a small spin parameter. In our model, the luminosity has a peak in the vicinity of the black hole, but is damped toward the event horizon and infinity. The power at the peak is of the same order as that in the Blandford–Znajek process, although the physical mechanism is different.

Key words: black hole physics – magnetic fields – plasmas – galaxies: active

1 INTRODUCTION

The Blandford–Znajek (BZ) process is widely discussed as a promising mechanism for the powerful central engines in active galactic nuclei, microquasars, and gamma ray bursts. In their seminal paper, Blandford & Znajek (1977) showed outgoing energy flux from the event horizon on the assumption of a steady force-free magnetosphere around a slowly rotating Kerr black hole. Owing to the simplified situation, the electromagnetic extraction of the rotational energy could be analytically demonstrated. This remarkable process has been studied, partly because the underlying assumptions are doubted and partly because realistic astrophysical relevance is very important.

Global steady-state force-free magnetospheres are constructed by numerically solving the relativistic Grad–Shafranov equation, in which there are singular surfaces that make careful treatment necessary (e.g., Uzdensky 2004, 2005; Contopoulos et al. 2013; Nathanail & Contopoulos 2014). Higher-order corrections to the original split monopole solution are calculated with respect to the black hole spin (e.g., Tanabe & Nagataki 2008; Pan & Yu 2015). The Grad–Shafranov equation for magnetohydrodynamics (MHD) equilibrium is much more complicated and difficult to solve (e.g., Takahashi et al. 1990; Nitta et al. 1991; Beskin & Par’ev 1993). A time-dependent approach may thus be preferable, and general relativis-

tic MHD simulations provide very interesting models (e.g., Koide et al. 2002; van Putten & Levinson 2003; Komissarov 2004b, 2005; McKinney 2006; Komissarov & Barkov 2009; McKinney et al. 2012). Recently, very complicated but more realistic configurations of the magnetic fields have been numerically treated. Of particular interest is the dynamical process in gamma ray bursts. The accretion of matter and jet emission in the vicinity of a central black hole can be explored simultaneously. Sometimes, transient features are also exhibited in the numerical simulations. Outgoing flow from a system of a black hole coupled with surrounding magnetic fields has been tested, but it is rather difficult to determine the most important elements from numerical results.

The mechanism for converting rotational energy to outgoing electromagnetic flux resembles that of a pulsar. However, the origin of electromotive force in a unipolar induction model is not established in the black hole magnetosphere. Possibilities include the event horizon (Thorne et al. (1986) and the critique by Punsly & Coroniti (1990)), ergosphere (Komissarov 2004a; Toma & Takahara 2014), and the pair creation surface (Beskin & Kuznetsova 2000; Okamoto 2012, 2015) (see also, (Punsly 2008; Beskin 2010) and the references therein). When the ideal MHD condition holds in the entire magnetosphere, the angular velocity Ω_F of the magnetic field is a function of magnetic flux, and this characterizes the electric potential difference between magnetic field lines. This value is crucial in the BZ mechanism, which works in only a certain range of Ω_F . There remain the problems of where and how it is specified. Toma & Takahara (2014)

[★] E-mail: ykojima-phys@hiroshima-u.ac.jp

argued that a breakdown of the ideal MHD condition in the ergosphere is essential for giving rise to electromotive force. However, their argument is qualitative by an almost analytic treatment. It is impossible to discuss the origin of electromotive force in the framework of the ideal MHD, and it is necessary to study it beyond the approximation level.

In this paper, we do not assume ideal MHD conditions; we instead consider a two-component plasma consisting of positively and negatively charged particles, whose flows are governed by electromagnetic fields and gravity. Maxwell's equations are solved with source terms of electric charge and current derived by the plasma motions, thus obtaining self-consistent solutions. Our approach allows us to explore the origin of the electromotive force and outgoing electromagnetic flux, if it exists. There are few works applying a two-fluid model to astrophysical situations, particularly to the formalism in black hole spacetime (Khanna 1998), and stationary pulsar models (Kojima & Oogi 2009; Petrova 2015). There are large numbers involved in the model to connect microscopic to macroscopic sizes, and this fact is an obstacle to numerical calculation.

This paper is organized as follows. Electromagnetic fields in a Kerr spacetime are discussed in Section 2 using 3 + 1 formalism. We provide a brief review, because the equations in many papers assume the ideal MHD condition and those without the condition are needed here. We also discuss plasma flows interacting with electromagnetic fields in curved spacetime. The equations of stream functions are derived. In Section 3, we present a model to investigate how black hole spin modifies plasma flows and electromagnetic fields, resulting in outgoing energy flux. In a Schwarzschild spacetime, both the flow and magnetic field are radial. That is, the magnetic field has a split-monopole configuration and the electric field vanishes. To consider slow rotation of the black hole, we adopt the perturbation technique and explicitly obtain the results. We present our conclusions in Section 4.

Note that in the following we assume axial symmetry and stationarity in electromagnetic fields and plasma flows. We use units of $c = G = 1$.

2 BASIC EQUATIONS

2.1 Electromagnetic fields

In this section, we briefly summarize the Maxwell equations in a black hole spacetime. The Kerr metric in the Boyer-Lindquist coordinate is given by

$$ds^2 = -\alpha^2 dt^2 + \frac{\rho^2}{\Delta} dr^2 + \rho^2 d\theta^2 + \varpi^2 (d\phi - \omega dt)^2, \quad (1)$$

where

$$\begin{aligned} \alpha^2 &= \frac{\rho^2 \Delta}{\Sigma^2}, \quad \rho^2 = r^2 + a^2 \cos^2 \theta, \quad \Delta = r^2 + a^2 - 2Mr, \\ \varpi^2 &= \frac{\Sigma^2}{\rho^2} \sin^2 \theta, \quad \Sigma^2 = (r^2 + a^2)^2 - a^2 \Delta \sin^2 \theta, \\ \omega &= \frac{2Mar}{\Sigma^2}. \end{aligned} \quad (2)$$

We consider stationary and axially symmetric fields, and the electromagnetic vectors \vec{E} and \vec{B} refer to quantities

measured by a locally non-rotating zero angular momentum observer (ZAMO). The four-velocity u^μ of a ZAMO in Boyer-Lindquist coordinates is given by

$$u^\mu = \frac{dx^\mu}{d\tau} = \left[\frac{1}{\alpha}, -\frac{1}{\alpha} \vec{\beta} \right], [\beta^{\hat{r}}, \beta^{\hat{\theta}}, \beta^{\hat{\phi}}] = [0, 0, -\omega \varpi]. \quad (3)$$

In this paper, the notation \hat{i} denotes the component of a vector in an orthogonal basis. Using vector analysis in a 3-dimensional curved space, the time-independent Maxwell equations are expressed as (e.g., Thorne et al. 1986)

$$\vec{\nabla} \cdot \vec{E} = 4\pi \rho_e, \quad (4)$$

$$\vec{\nabla} \cdot \vec{B} = 0, \quad (5)$$

$$\vec{\nabla} \times (\alpha \vec{E}) = (\vec{\beta} \cdot \vec{\nabla}) \vec{B} - (\vec{B} \cdot \vec{\nabla}) \vec{\beta}, \quad (6)$$

$$\vec{\nabla} \times (\alpha \vec{B}) = 4\pi \alpha \vec{j} - (\vec{\beta} \cdot \vec{\nabla}) \vec{E} + (\vec{E} \cdot \vec{\nabla}) \vec{\beta}. \quad (7)$$

It is convenient to introduce three scalar functions $G(r, \theta)$, $S(r, \theta)$, and $\Phi(r, \theta)$ to express these fields. These respectively represent the magnetic flux, poloidal current flow, and electric potential¹. The following forms satisfy eqs. (5) and (6):

$$\vec{B} = \frac{\vec{\nabla} G \times \vec{e}_{\hat{\phi}}}{\varpi} + \frac{S}{\alpha \varpi} \vec{e}_{\hat{\phi}}, \quad (8)$$

$$\vec{E} = -\frac{1}{\alpha} \vec{\nabla} \Phi - \frac{\vec{\beta}}{\alpha} \times \vec{B} = -\frac{1}{\alpha} (\vec{\nabla} \Phi - \omega \vec{\nabla} G). \quad (9)$$

Their components are explicitly written as

$$[B_{\hat{r}}, B_{\hat{\theta}}, B_{\hat{\phi}}] = \left[\frac{1}{\varpi \rho} G_{,\theta}, -\frac{\Delta^{1/2}}{\varpi \rho} G_{,r}, \frac{S}{\alpha \varpi} \right], \quad (10)$$

$$[E_{\hat{r}}, E_{\hat{\theta}}, E_{\hat{\phi}}] = \left[-\frac{\Delta^{1/2}}{\alpha \rho} (\Phi_{,r} - \omega G_{,r}), -\frac{1}{\alpha \rho} (\Phi_{,\theta} - \omega G_{,\theta}), 0 \right] \quad (11)$$

Since $E^2 - B^2 = ((\omega \varpi / \alpha)^2 - 1) |\nabla G / \varpi|^2$, it is easily found that the electric fields dominate inside the ergoregion if the toroidal magnetic fields and longitudinal electric fields vanish ($S = \Phi = 0$). Equivalently, the magnitude of ' $\vec{E} \times \vec{B}$ ' drift velocity v_d exceeds the speed of light inside the ergoregion, $|v_d| = |\vec{E} \times \vec{B}| / B^2 = |\omega \varpi / \alpha| > 1$. This indicates a breakdown of the MHD condition (Toma & Takahara 2014). As a result, longitudinal electric fields arise to redistribute charge density.

The poloidal component (r, θ) of eq. (7) is given by

$$4\pi \alpha \vec{j}_p = \frac{\vec{\nabla} S \times \vec{e}_{\hat{\phi}}}{\varpi}. \quad (12)$$

¹ In the literature, symbols such as Φ , Ψ , A , or f are used instead of G , and the electric potential is related by the ideal MHD condition. We do not assume this condition, so a new set of symbols is used here.

The poloidal current flows along a constant line S . The toroidal component (ϕ) of eq. (7) is

$$\mathcal{D}G + \frac{\varpi^2}{\alpha\rho^2} [\omega_{,r}\Delta(\Phi_{,r} - \omega G_{,r}) + \omega_{,\theta}(\Phi_{,\theta} - \omega G_{,\theta})] = -4\pi\alpha\varpi j_{\phi}, \quad (13)$$

where \mathcal{D} is a differential operator given by

$$\begin{aligned} \mathcal{D}G &= \varpi^2 \vec{\nabla} \cdot \left(\frac{\alpha}{\varpi^2} \vec{\nabla} G \right) \\ &= \frac{\Delta^{1/2} \varpi}{\rho^2} \left[\left(\frac{\alpha \Delta^{1/2}}{\varpi} G_{,r} \right)_{,r} + \left(\frac{\alpha}{\varpi \Delta^{1/2}} G_{,\theta} \right)_{,\theta} \right] \end{aligned} \quad (14)$$

Finally, Gauss' law (4) is explicitly written as

$$\begin{aligned} \frac{\Delta^{1/2}}{\rho^2 \varpi} \left[\left(\frac{\Delta^{1/2} \varpi}{\alpha} (\Phi_{,r} - \omega G_{,r}) \right)_{,r} \right. \\ \left. + \left(\frac{\varpi}{\alpha \Delta^{1/2}} (\Phi_{,\theta} - \omega G_{,\theta}) \right)_{,\theta} \right] = -4\pi\rho_e. \end{aligned} \quad (15)$$

Once the electromagnetic fields are known, the outgoing energy flux through a surface at a radius r is calculated as follows (see the Appendix):

$$P_{\text{em}}(r) = - \int (\sqrt{-g} T_{\text{em}}^r{}_t) d\theta d\phi = - \frac{1}{2} \int (\Phi_{,\theta} S) d\theta. \quad (16)$$

In the above we have presented a general form of stationary and axially symmetric electromagnetic fields, which are described by three functions. If the ideal MHD condition $\vec{E} \cdot \vec{B} = 0$ holds, we have $\Phi = \Phi(G)$, or $\vec{\nabla}\Phi = \Omega_F(G) \vec{\nabla}G$, where Ω_F represents the angular velocity of the magnetic field. Moreover, when the force-free approximation $\rho_e \vec{E} + \vec{j} \times \vec{B} = 0$ is used, the azimuthal component leads to $S = S(G)$. The electromagnetic fields are described only by the magnetic function G (the Grad-Shafranov equation). The number of differential equations decreases, but there remains the problem of specifying their functional relations, $\Omega_F(G)$ and $S = S(G)$.

2.2 Outgoing energy flux from horizon

To evaluate P_{em} in eq. (16) near a black hole horizon (at $r_H = M + \sqrt{M^2 - a^2}$), we need the behavior of the functions Φ and S . For a while, we assume that the ideal MHD condition holds, that is, $\Phi_{,\theta} = \Omega_F G_{,\theta}$. Near the horizon, the function S is specified by imposing the so-called Znajek condition (Znajek 1978), $B_{\hat{\phi}} = -E_{\hat{\theta}}$, which is written from eqs. (10),(11) as

$$S = (\Phi_{,\theta} - \omega_H G_{,\theta}) \frac{\varpi}{\rho}, \quad (17)$$

where $\omega_H \equiv \omega(r_H) = a/(2Mr_H)$ is the angular velocity of the black hole. This condition is equivalent to the incoming electromagnetic wave (Thorne et al. 1986). By substituting these expressions into eq. (16), the outgoing electromagnetic power is

$$P_{\text{em}}(r_H) = - \frac{1}{2} \Omega_F (\Omega_F - \omega_H) \int_{r_H} \frac{\varpi}{\rho} (G_{,\theta})^2 d\theta. \quad (18)$$

This shows that the power $P_{\text{em}}(r_H)$ is positive when $0 < \Omega_F < \omega_H$. This is the outgoing energy flux from a rotating black hole in the BZ process. A remaining problem is how the angular velocity Ω_F of the magnetic field lines or equivalently the longitudinal electric potential Φ is determined.

2.3 Fluid

We adopt a treatment in which the plasma is modeled as a two-component fluid. Each component, consisting of positively or negatively charged particles, is described by a number density n_{\pm} and velocity \vec{v}_{\pm} , which denote the values measured by a ZAMO. The proper density n_{\pm}^* measured in the fluid rest frame is related to n_{\pm} and a Lorentz factor $\gamma_{\pm} = (1 - (v_{\pm}/c)^2)^{-1/2}$ by $n_{\pm}^* = (n/\gamma)_{\pm}$, where an abbreviation $(n/\gamma)_{\pm} \equiv n_{\pm}/\gamma_{\pm}$ is introduced. We assume that the positive particle has mass m and charge e , while the negative one has mass m and charge $-e$. The charge density and electric current are given in terms of n_{\pm} and \vec{v}_{\pm} as

$$\rho_e = e(n_+ - n_-), \quad (19)$$

$$\vec{j} = e(n_+ \vec{v}_+ - n_- \vec{v}_-). \quad (20)$$

The continuity equation for each component in the axisymmetric stationary condition is

$$0 = \vec{\nabla} \cdot (\alpha n^* \gamma \vec{v}_p)_{\pm} = \vec{\nabla} \cdot (\alpha n \vec{v}_p)_{\pm}, \quad (21)$$

where the factor α comes from the relation between the determinant of 4-dimensional spacetime metrics and that of 3-dimensional space $\sqrt{-g_4} = \alpha \sqrt{g_3}$. This equation is satisfied by introducing a stream function $F_{\pm}(r, \theta)$ as

$$\alpha(n \vec{v}_p)_{\pm} = \frac{1}{\varpi} \vec{\nabla} F_{\pm} \times \vec{e}_{\hat{\phi}}. \quad (22)$$

From this definition, the number density is solved as

$$\begin{aligned} n_{\pm} &= (\alpha \varpi)^{-1} (|\nabla F| (v_r^2 + v_{\theta}^2)^{-1/2})_{\pm} \\ &= (\alpha \varpi)^{-1} (|\nabla F| (1 - \gamma^{-2} - v_{\phi}^2)^{-1/2})_{\pm}. \end{aligned} \quad (23)$$

From eqs. (20) and (22), the current flow function S of eq. (12) can be given by

$$S = 4\pi e (F_+ - F_-). \quad (24)$$

The law of momentum conservation in a stationary axially symmetric state (Khanna 1998) is

$$\frac{1}{\alpha} \nabla_j (\alpha T_{\pm}^j{}_i) = \rho_{\text{m}\pm} g_i + H_{ij} S_{\text{m}\pm}^j \pm e n_{\pm}^* \gamma_{\pm} (\vec{E} + \vec{v}_{\pm} \times \vec{B})_i \pm (R_{\text{col}})_i, \quad (25)$$

where the first term denotes gravitational acceleration with $\vec{g} \equiv -\vec{\nabla} \ln \alpha$, the second is a gravito-magnetic term with $H_{ij} \equiv \alpha^{-1} \nabla_i \beta_j$, the third is the electromagnetic force, and the last is the collision term. Here we consider the cold limit, so that thermal pressure is ignored, and the stress tensor is $T_{\pm}^{ij} = (m n^* \gamma^2 v^i v^j)_{\pm}$, energy density $\rho_{\text{m}\pm} = (m n^* \gamma^2)_{\pm}$, and momentum flux $S_{\text{m}\pm}^i = (m n^* \gamma^2 v^i)_{\pm}$. Moreover, we neglect the collision term. As Khanna (1998) discussed, near the black hole horizon, the electron collision time becomes longer than the dynamical timescale, so the collisionless approximation may be valid under certain conditions. Using the collision rate ν_c (Spitzer 1962) and free-fall timescale t_{ff} , the product is $\nu_c t_{\text{ff}} \sim 10^{-3}$, where the electron number density $n_e \sim 10^{16} (\dot{M}/10^{-2} \dot{M}_{\text{E}}) (M/M_{\odot})^{-1} \text{ cm}^{-3}$, estimated from the accretion rate, and thermal velocity at $T = 10^{12} \text{ K}$ are used. Collisions are ignored in the dilute approximation. Thus, the equation of motion (25) for each component through the global electromagnetic and gravitational forces is reduced to

$$[(\vec{\nabla} \times \gamma \vec{v}) \times \vec{v} + \vec{\nabla} \gamma]_{\pm i} = \gamma_{\pm} g_i + H_{ij} (\gamma v^j)_{\pm} \pm \frac{e}{m} [\vec{E} + \vec{v}_{\pm} \times \vec{B}]_i,$$

(26)

where the left-hand side is written in the vector form. From eq. (26), it is clear that there are two conserved quantities along each stream line, namely, the generalized angular momentum J_{\pm} and the Bernoulli integral K_{\pm} , which are equivalent to u_{ϕ} and u_t for each fluid component:

$$J_{\pm} = (\omega\gamma v_{\phi})_{\pm} \pm \frac{e}{m}G, \quad (27)$$

$$K_{\pm} = (\omega\gamma v_{\phi})_{\pm} + \alpha\gamma_{\pm} \pm \frac{e}{m}\Phi. \quad (28)$$

These quantities depend on only the stream functions F_{\pm} , and the spatial distributions are therefore determined by F_{\pm} , which is specified at the injection point in our model. The component of eq. (26) perpendicular to the stream lines gives

$$\begin{aligned} \alpha\varpi^2\vec{\nabla} \cdot \left(\frac{\gamma_{\pm}}{\alpha n_{\pm}\varpi^2}\vec{\nabla}F_{\pm} \right) \\ = \alpha\varpi^2 n_{\pm} \left(K'_{\pm} - (v_{\phi}^{\pm} + w_0) \frac{\alpha}{\varpi} J'_{\pm} \right) \pm \frac{e}{m}S, \end{aligned} \quad (29)$$

where $w_0 = \omega\varpi/\alpha$, and J'_{\pm} and K'_{\pm} are derivatives of J_{\pm} and K_{\pm} with respect to F_{\pm} .

We have thus obtained a system of equations that govern the electromagnetic field structure and plasma flows. Four partial differential equations (13), (15), (29) should be solved with two integrals (27), (28) and the number density (23) derived by the stream functions. These are reduced to those obtained for pulsar electrodynamics in a flat spacetime (Kojima & Oogi 2009) by setting $M = a = 0$. These equations for G , Φ , and F_{\pm} are interdependent in a nonlinear manner, so iterative methods are needed to self-consistently solve a set of these equations. For example, assume that functions G , Ψ , and F_{\pm} are known. The azimuthal velocity v_{ϕ} and Lorentz factor γ are determined by the integrals in Eqs. (27) and (28). The number density is calculated from eq. (23). Thus, the source terms, namely, the toroidal current j_{ϕ} in eq. (13) and the charge density ρ_e in eq. (15), are calculated from the fluid quantities of both species. The source terms and complicated coefficients in the equation of F_{\pm} are also calculated. A new set of functions is solved for these source terms with appropriate boundary conditions. This procedure is repeated until convergence.

3 MODEL DESCRIPTION

3.1 Parameters and normalization

We now describe a general framework for determining the electromagnetic fields and charged flows described in the previous section. Here, we discuss physical parameters involved in our system.

There are two independent parameters. One is a dimensionless gyrofrequency, $\chi \equiv \omega_B M = eB_0 M/m$, where B_0 is a typical magnetic field strength. Associated with B_0 is a characteristic number density $n_c \equiv B_0/(4\pi eM)$. The number density is reduced to the so-called Goldreich-Julian density if the timescale $2M$ is replaced by the stellar angular velocity Ω_s^{-1} . The actual number density is normalized by λn_c , where λ represents the multiplicity of pair plasma.

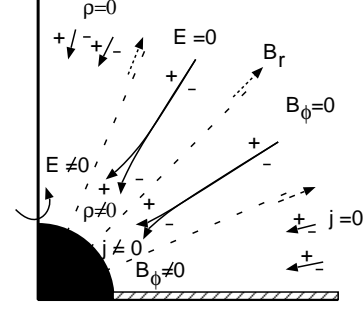


Figure 1. A schematic illustration for electromagnetic fields and plasma inflows around a rotating black hole. The magnetic field is radial without toroidal component, and electric field vanishes in the outer region. Black hole rotation affects the plasma flow, and a new electromagnetic structure is induced in the inner region. There is a current sheet on an equator to support the split-monopole magnetic field.

We can express other physically meaningful quantities using these dimensionless parameters χ and λ . The normalized plasma frequency κ with number density λn_c is given by $\kappa^2 \equiv \omega_p^2 M^2 = 4\pi e^2 (\lambda n_c) M^2 / m = \lambda \chi$. The ratio of λ to χ is written as $k \equiv \lambda/\chi = (1/4) \times (2m\lambda n_c)/(B_0^2/8\pi)$, and represents the ratio of the rest mass energy density of pairs to the electromagnetic energy density. These numbers χ and λ are very large in astrophysical situations. A typical value of χ is $10^{13}(B_0/\text{kG})(M/10^8 M_{\odot})$, relevant to active galactic nuclei powers $\propto (MB_0)^2$. The amount of pair plasma is unclear, but we here estimate it from the accretion rate \dot{M} . Using the electron number density $n_e \sim 10^8 (\dot{M}/10^{-2} \dot{M}_E)(M/10^8 M_{\odot})^{-1} \text{ cm}^{-3}$ near the horizon, we have $\kappa^2 = 10^{22} (\dot{M}/10^{-2} \dot{M}_E)(M/10^8 M_{\odot})$. The other parameters are calculated as $\lambda = \kappa^2/\chi \sim 10^9$ and $k = \kappa^2/\chi^2 \sim 10^{-4}$. See also Beskin (2010) for estimates for microquasars and gamma ray bursts, for which $\lambda \sim 10^{10} - 10^{14}$. It is true that $\lambda, \chi, \kappa^2 \gg 1$, but these values should be regarded as an order estimate with large uncertainties. In particular, the ratio $k = \lambda/\chi$ may drastically change in the cases of matter-dominated or magnetically dominated flows. Indeed, the activation condition of the BZ mechanism in the MHD flows is approximately given by $k < 1$, for which the Alfvén speed exceeds the free-fall velocity at the ergosphere (Komissarov & Barkov 2009). Magnetization parameter corresponds to $1/k$.

We provide an explicit model of electromagnetic fields and plasma inflows in a hemisphere ($0 \leq \theta \leq \pi/2$), depicted schematically in Fig. 1. We assume that the electromagnetic fields at $r_{\text{out}} \gg M$ are described by $\vec{B} = B_0(M/r)^2 \vec{e}_r$, $B_{\phi} = 0$ and $\vec{E} = 0$, where B_0 is a constant representing magnetic field strength. This condition differs from the wind solution by Michel (1973) in which toroidal magnetic field and electric fields are given by $B_{\phi} = E_{\theta} = -\Omega_F B_0 M^2 \sin \theta / r$. Our concern is how the parameter Ω_F is determined, so that the condition $\Omega_F = 0$ is used at r_{out} . Such a split-monopole magnetic field may be formed by strong currents on an equatorial disk, by which upper and lower hemispheres are detached. The electromagnetic fields are obtained by the derivatives of $\vec{G} \equiv G/(B_0 M^2) = (1 - \cos \theta)$, $\vec{S} \equiv S/(B_0 M) = 0$ and $\vec{\Phi} \equiv \Phi/(B_0 M) = 0$, where \vec{G} , \vec{S} and $\vec{\Phi}$ are normalized dimensionless quantities.

As for the pair plasma, we assume neutral flow falling along the radial magnetic fields at $r_{\text{out}} \gg M$, that is, $v_{\phi}^{\pm} \rightarrow 0$ and $\alpha\gamma_{\pm} \rightarrow 1$. The stream functions F_{\pm} of both components should coincide there, since $F_+ - F_- = S/(4\pi e) = 0$ in eq. (24). Like the magnetic function G , both functions are chosen to be radial, $F_{\pm} = -\lambda n_c M^2(1 - \cos \theta)$, where $n_c \equiv B_0/(4\pi e M)$ is a characteristic number density and the minus sign denotes inflow $v_{\hat{r}}^{\pm} < 0$. We introduce dimensionless stream functions $\bar{F}_{\pm} = F_{\pm}/(\lambda n_c M^2)$ and the dimensionless number density $\bar{n}_{\pm} = n_{\pm}/(\lambda n_c)$. The relation (24) between \bar{S} and \bar{F}_{\pm} becomes $\bar{S} = \lambda(\bar{F}_+ - \bar{F}_-)$.

Under these conditions at r_{out} , the integrals J_{\pm} and K_{\pm} in eqs. (27) and (28) are explicitly given by

$$J_{\pm} = \mp \frac{\chi}{\lambda n_c M} F_{\pm} = \mp \chi M \bar{F}_{\pm}, \quad K_{\pm} = \alpha\gamma_{\pm} = 1, \quad (30)$$

where the Lorentz factor at $r_{\text{out}} (\gg M)$ is for simplicity chosen as $\gamma_{\pm} = \alpha^{-1} (\approx 1)$. Once J_{\pm} is specified, the azimuthal velocity v_{ϕ}^{\pm} can be solved at any point from eq. (27) as

$$v_{\phi}^{\pm} = \mp \frac{\chi M}{\varpi \gamma_{\pm}} (\bar{F}_{\pm} + \bar{G}). \quad (31)$$

The Lorentz factor γ_{\pm} can also be solved from eq. (28) as

$$\alpha\gamma_{\pm} = 1 \pm \chi [\omega M (\bar{F}_{\pm} + \bar{G}) - \bar{\Phi}]. \quad (32)$$

Since we have $K'_{\pm} = 0$ and $J'_{\pm} = \mp \chi/(\lambda n_c M)$, eq. (29) is reduced to

$$\alpha \varpi^2 \vec{\nabla} \cdot \left(\frac{M^2 \gamma_{\pm}}{\alpha \bar{n}_{\pm} \varpi^2} \vec{\nabla} \bar{F}_{\pm} \right) = \pm \chi \left[\frac{\alpha^2 \varpi \bar{n}_{\pm}}{M} (w_0 + v_{\phi}^{\pm}) + \bar{S} \right], \quad (33)$$

where $w_0 = \omega \varpi / \alpha$.

In this model, we have imposed the conditions $S = 0$ and $\Phi = 0$ at r_{out} , so the electromagnetic Poynting power (16) is zero ($P_{\text{em}}(r_{\text{out}}) = 0$). If the ideal MHD condition holds in $r_{\text{H}} \leq r \leq r_{\text{out}}$, then we have $\Phi = 0$ everywhere, including the black hole horizon as the asymptotic limit, since the constant Ω_{F} along any magnetic field line is zero. Consequently, no electromagnetic power is produced. Our concern is how power is produced in the presence of black hole spin. For this purpose, we have to consider non-ideal MHD effects.

3.2 Spherical flow

Here, we discuss the structure of the electromagnetic field and plasma flows in Schwarzschild spacetime. An analytic solution is given in terms of dimensionless functions as

$$\bar{G} = -\bar{F}_{\pm} = 1 - \cos \theta, \quad \bar{\Phi} = \bar{S} = 0. \quad (34)$$

The electromagnetic fields are explicitly written as

$$[B_{\hat{r}}, B_{\hat{\theta}}, B_{\hat{\phi}}] = \left[\frac{B_0 M^2}{r^2}, 0, 0 \right], \quad [E_{\hat{r}}, E_{\hat{\theta}}, E_{\hat{\phi}}] = [0, 0, 0]. \quad (35)$$

The flow velocity, its Lorentz factor, and number density of the flow are given by

$$\begin{aligned} [v_{\hat{r}}^{\pm}, v_{\hat{\theta}}^{\pm}, v_{\hat{\phi}}^{\pm}] &= \left[-\left(\frac{2M}{r} \right)^{1/2}, 0, 0 \right], \\ \gamma_{\pm} &= \gamma_0 = (1 - (v_{\pm})^2)^{-1/2} = \alpha^{-1}, \\ \bar{n}_0 &\equiv \frac{n_{\pm}}{\lambda n_c} = \frac{1}{\sqrt{2}} \frac{M^{3/2}}{\sqrt{r^2(r-2M)}}. \end{aligned} \quad (36)$$

The number density n_{\pm} appears to diverge at the horizon $r \rightarrow 2M$, but the proper density $n_{*\pm} = n_{\pm}/\gamma_0$ is finite everywhere, as $n_{\pm}/(\lambda n_c \gamma_0) = M^{3/2}/(\sqrt{2}r^{3/2})$. The proper density and the magnetic field strength at $r = 2M$ are $n_{*\pm} = \lambda n_c/4$, and $B_{\hat{r}} = B_0/4 \equiv B_{\text{n}}$. Thus, B_0 and λn_c are reasonable values near the black hole horizon, estimated in the previous section.

This is a spherically symmetric solution, so that the conditions imposed at radius r_{out} are retained everywhere. In particular, the electromagnetic power is zero everywhere. The energy flow P_0 of matter across a sphere with radius r is obtained by twice the value in a hemisphere ($0 \leq \theta \leq \pi/2$):

$$P_0 = -2 \times 4\pi \lambda n_c m M^2 = -\frac{2\lambda}{\chi} B_0^2 M^2. \quad (37)$$

Here, a minus sign denotes inflow, and the factor 2 comes from summing the contribution of positively and negatively charged fluids (see the Appendix).

3.3 Effect of slow rotation

We examine the effect of black hole spin on the spherical flow given by eqs. (34)–(36). It is rather difficult numerical work to obtain consistent solutions for G , Φ , and F_{\pm} in eqs. (13), (15), and (33), as they consist of nonlinearly coupled partial differential equations. We here consider the rotation as a small parameter, and expand these functions as, for example, $F_{\pm} = \lambda n_c M^2 (\bar{F} + \delta F_{\pm})$. We limit our consideration to the first-order effect. The Poynting flux given by eq. (16) is a product of $\Phi_{,\theta}$ and S . Both are zero for $a = 0$, but are modified by the first-order rotational effect. Poynting flux is thus produced within this approximation level. Within the first-order effect of the black hole spin, the only difference from the Schwarzschild metrics is the function ω , which is approximated as $\omega = 2M^2 a_* r^{-3}$, where $a_* = a/M$ is a dimensionless Kerr parameter. We assume $a_* > 0$, which determines the direction of perturbed vectors. In this section, the symbols α and ϖ denote those for $a_* = 0$, that is, $\alpha^2 = 1 - 2M/r$ and $\varpi = r \sin \theta$.

We next develop the perturbation equations. We first note that the rotational effect in eq. (33) is the term $w_0 = \alpha^{-1} \omega \varpi$ in only the lowest approximation, and that the term in the equation of the stream functions F_{\pm} works in an opposite direction with respect to the fluid species. We therefore consider only a class of perturbations $\delta F_+ = -\delta F_-$. From the perturbation of eq. (31), δv_{ϕ}^{\pm} is expressed by δF^{\pm} and δG , but after careful consideration we conclude that $\delta G = 0$ and $\delta v_{\phi}^{\pm} = \delta v_{\phi}^{\mp}$. We also have $\delta G = 0$ in the perturbation of eq. (13), consistent with $0 = \delta j_{\phi}^{\pm} \propto (\delta v_{\phi}^+ - \delta v_{\phi}^-)$. From now on, we will use a function $\delta F \equiv \delta F_+ = -\delta F_-$, and δv_{ϕ}^{\pm} is given by

$$\delta v_{\phi}^{\pm} = -\chi M (\varpi \gamma_0)^{-1} \delta F. \quad (38)$$

Under these conditions the perturbation of eq. (32) is reduced to

$$\delta \gamma^{\pm} = \mp \chi \alpha^{-1} \delta \Phi = \mp \chi \gamma_0 \delta \Phi. \quad (39)$$

The acceleration, which is opposite that of the fluid species, originates from the perturbation of electric potential. The perturbation of number density, eq. (23), is also

opposite to the species and is given by

$$\frac{\delta n_{\pm}}{\bar{n}_0} = \pm \left[-\frac{1}{\sin \theta} \delta F_{,\theta} + \chi(\gamma_0^2 - 1)^{-1} \delta \Phi \right]. \quad (40)$$

Finally, we consider the perturbation equations for $\delta \Phi$ and δF . General forms expanded with the Legendre polynomials $P_l(\theta)$ are given by $\delta \Phi = \sum h_l(r) P_l(\theta)$ and $\delta F = -\sum (l+1)^{-1} p_l(r) P_{l,\theta}(\theta) \sin \theta$. The slow rotation corresponds to the dipole perturbation with $l = 1$, so that the components with $l \neq 1$ are decoupled with the rotational perturbation. Therefore we have $\delta \Phi = h(r) \cos \theta$ and $\delta F = (1/2)p(r) \sin^2 \theta$. Substituting their forms into the perturbation equations of Eqs. (15) and (33), after some manipulations we derive the following:

$$\frac{\alpha^2}{s^2} \frac{d}{ds} \left(s^2 \frac{dh}{ds} \right) = - \left[\frac{\kappa^2 \alpha^2}{\sqrt{2}s} - \frac{2}{s^2} \right] h + \frac{\sqrt{2}\lambda}{s^{3/2}} p + \frac{4a_*}{s^5}, \quad (41)$$

$$\alpha^2 \frac{d}{ds} \left(\frac{s^{3/2}}{\alpha^2} \frac{dp}{ds} \right) = \left[\sqrt{2}\kappa^2 - \frac{\chi^2 \alpha^2}{2s^{3/2}} \right] p + \chi s^{1/2} h + \frac{2\chi a_*}{s^{5/2}}. \quad (42)$$

Here, we use normalized radial coordinate $s \equiv r/M$. We thus have a coupled set of second-order ordinary differential equations. There are very large numbers involved in the first terms on the right-hand side, namely the squares of the plasma frequency κ and gyrofrequency χ . The last terms represent the effect of black hole spin a_* . Our concern is the range $\chi \gg 1$ and $\kappa^2 = \lambda\chi \gg 1$, but $k = \lambda/\chi$ is not so large. Replacing $\kappa^2 = k\chi^2$ in eqs. (41) and (42), we neglect higher order terms of χ^{-n} ($n > 2$) except the derivative terms. Thus, eqs. (41) and (42) are approximated in forms suitable for WKB analysis:

$$\left[\chi^{-2} \frac{d^2}{ds_*^2} + U \right] \left(\frac{sh}{\alpha} \right) - \chi^{-1} \sqrt{2}kA \left(\frac{s^{3/4}p}{\alpha^2} \right) = 0, \quad (43)$$

$$\left[\chi^{-2} \frac{d^2}{ds_*^2} - V \right] \left(\frac{s^{3/4}p}{\alpha^2} \right) - \chi^{-1}A \left(\frac{sh}{\alpha} \right) = \chi^{-1}J_s. \quad (44)$$

Here, s_* in eqs. (43)–(44) denotes tortoise coordinate $s_* \equiv r_*/M = (r/M) + 2 \log(r/2M - 1)$ satisfying $ds_*/ds = \alpha^{-2}$. Other terms in eqs. (43)–(44) are

$$U = (k/\sqrt{2})\alpha^4 s^{-1/2}, \quad V = \left(\sqrt{2}k - \frac{1}{2}\alpha^2 s^{-3/2} \right) \alpha^4 s^{-3/2}, \\ A = \alpha^3 s^{-5/4}, \quad J_s = 2a_*\alpha^2 s^{-13/4}. \quad (45)$$

The system of Eqs. (43)–(44) is rather simplified, since the source term in eq. (43), the higher order term $\sim \chi^{-2}$, is neglected, and the potential terms U and V involve a parameter $k = \lambda/\chi$.

3.4 WKB solutions

We first consider the homogeneous solution of eqs. (43)–(44). We seek an approximate solution of the WKB form $p \propto \exp(\chi W(s))$ and $h \propto \exp(\chi W(s))$, where $\chi^{-1} (\ll 1)$ is a small WKB parameter. Substituting them in, we find the leading-order solutions correct to order χ^{-1} . The four

independent solutions (two pairs) given below are denoted by h_n^{\pm}, p_n^{\pm} . Two types are clearly distinguished among the three points: (1) oscillatory or growing/decaying behaviors, (2) the relative ordering between h and p and (3) their relative sign. A pair of type I solutions is given by

$$h_I^{\pm} = \alpha s^{-1} U^{-1/4} \exp(\pm i\chi \int^{s_*} U^{1/2} ds'_*) \\ = 2^{1/8} k^{-1/4} s^{-7/8} \exp(\pm i\kappa_1 s^{3/4}), \quad (46)$$

$$p_I^{\pm} = -2\chi^{-1} s^{1/2} \left[2^{1/2} k(s+2) - \alpha^2 s^{-3/2} \right]^{-1} h_I^{\pm}, \quad (47)$$

where $\kappa_1 = (2^{7/4}/3)\kappa$ and an overall constant from the integral is adjusted in eq. (46). The solution represents spatial oscillation of the plasma, whose wavelength is $\sim \kappa^{-1}M$. The solution satisfies the relations $p_I^{\pm} \sim \chi^{-1} \times h_I^{\pm} \ll h_I^{\pm}$ in the large χ limit, and $h_I^{\pm} p_I^{\pm} < 0$ if the value in square brackets in eq. (47) is positive. The last condition is satisfied when $k = \lambda/\chi > 9.1 \times 10^{-3}$. The functions h_I^{\pm} and p_I^{\pm} are regular toward the black hole horizon $\alpha \rightarrow 0, r \rightarrow 2M$.

Another pair of type II solutions is

$$p_{II}^{\pm} = \alpha^2 s^{-3/4} V^{-1/4} \exp(\pm \chi \int^{s_*} V^{1/2} ds'_*), \quad (48)$$

$$h_{II}^{\pm} = 2^{3/2} \chi^{-1} k \alpha^{-2} \left[2^{1/2} k(s+2) - \alpha^2 s^{-3/2} \right]^{-1} p_{II}^{\pm}. \quad (49)$$

Here, we assume that V is positive everywhere. This condition is satisfied for the parameter $k = \lambda/\chi > k_c$, $k_c \approx 2.3 \times 10^{-2}$. When $k < k_c$ the potential V becomes negative in some range $r_1 < r < r_2$, and the function in eq. (48) becomes oscillatory there. A whole solution is obtained by matching functions at r_1 and r_2 . We expect that such a solution is possible for only a discrete value of k , namely, an eigenvalue, and requires more careful treatment. In the following, our consideration is limited to the case $k > k_c$. Note that values in the square brackets in eqs. (47) and (49) are positive for that case as well.

For later convenience, we approximate the integral in the exponential in eq. (48). With a constant $\kappa_2 = 2^{9/4}\kappa$, eq. (48) is reduced to

$$p_{II}^{\pm} \approx 2^{-1/8} k^{-1/4} \alpha s^{-3/8} \exp(\pm \kappa_2 s^{1/4}). \quad (50)$$

We numerically verified that the approximation is good so long as $\kappa \gg 1$ and $k > k_c$.

We next discuss properties of the type II solutions in eqs. (48) and (49). These are exponentially growing/decaying functions with a relation $h_{II}^{\pm} \sim \chi^{-1} \times p_{II}^{\pm} \ll p_{II}^{\pm}$ in the large χ limit. This ordering is opposite to that in h_I^{\pm} and p_I^{\pm} . As discussed in the next subsection, the sign of $h_{II}^{\pm} p_{II}^{\pm} > 0$ is critical for outgoing energy power. The function $p_{II}^{\pm} \propto \alpha$ goes to zero at the horizon $\alpha \rightarrow 0$, while h_{II}^{\pm} in general diverges as $h_{II}^{\pm} \sim \alpha^{-1}$. The divergence in h_{II} will be eliminated by appropriate combination of p_{II}^{\pm} , as discussed below.

A general solution of eqs. (43) and (44) without the source term J_s is expressed by a linear combination of four functions as $h = \sum c_n^{\pm} h_n^{\pm}(s)$, and $p = \sum c_n^{\pm} p_n^{\pm}(s)$. The solution of the inhomogeneous equation is obtained by varying the coefficients c_n^{\pm} as $h = \sum c_n^{\pm}(s) h_n^{\pm}(s)$, and $p = \sum c_n^{\pm}(s) p_n^{\pm}(s)$. We put these forms into eqs. (43) and

² The form δF allows stream lines to hit on the equator, and therefore poloidal current may go into and out it. This point will be discussed later.

(44), and find that $dc_{\text{II}}^{\pm}/ds_* \propto \chi^{-1}$ and that the functions c_{II}^{\pm} satisfy the following equation of order χ^0 :

$$\frac{dc_{\text{II}}^{\pm}}{ds_*} = \pm \frac{1}{2} \frac{J_s}{V^{1/4}} \exp(\mp \chi \int^{s_*} V^{1/2} ds'_*). \quad (51)$$

We neglect corrections to the type I solution, and consider only the effect of source term J_s on c_{II}^{\pm} . By integrating eq. (51), a particular solution of the inhomogeneous equation is written in a concise form as

$$p_{\text{II}}^{\text{S}} = -\frac{a_* \alpha^2}{s^{3/4} V^{1/4}} \int_{\text{in}}^{\text{out}} \frac{\alpha^2}{\xi^{13/4} V^{1/4}} \exp(-\chi |\int_{\xi}^s V^{1/2} \alpha^{-2} ds'|) d\xi \quad (52)$$

$$\approx -\frac{a_* \alpha}{2^{1/4} k^{1/2} s^{3/8}} \int_{\text{in}}^{\text{out}} \alpha^{-1} \xi^{-23/8} \exp(-\kappa_2 |s^{1/4} - \xi^{1/4}|) d\xi. \quad (53)$$

This is a method to solve inhomogeneous equations in terms of a Green function constructed by the WKB approximation (see, e.g., [Bender & Orszag 1999](#)).

The solution p of eqs. (43) and (44) is in general a sum of p_{II}^{S} and p_{II}^{\pm} , a growing solution p_{II}^+ is ignored since $\kappa r_{\text{out}}/M \gg 1$. Even if small value $p_{\text{II}}^+(r_{\text{out}})$ may be involved, the contribution exponentially decreases with the decrease of r . The regular solution both at the horizon and at infinity is given with a constant c_{II}^- by

$$p = p_{\text{II}}^{\text{S}} + c_{\text{II}}^- p_{\text{II}}^-. \quad (54)$$

The solution h ($\sim \chi^{-1} p$) is obtained by the relation (49), which may be unchanged within the lowest approximation. Both p_{II}^{S} and p_{II}^- go to zero toward the horizon, $p_{\text{II}}^{\text{S}}, p_{\text{II}}^- \propto \alpha^1 \rightarrow 0$, whereas h_{II} diverges in general as $h_{\text{II}} \propto \alpha^{-1}$. The regularity condition is $\delta E_{\hat{r}} = -\delta \Phi_{,r} \sim \alpha^0$ and $\delta E_{\hat{\theta}} = -(\alpha r)^{-1} (\delta \Phi_{,\theta} - \omega G_{,\theta}) \sim \alpha^{-1}$ in ZAMO variables ([Thorne et al. 1986](#)). This means that the function h_{II} should be finite at the horizon, and therefore the constant c_{II}^- may be uniquely determined as $c_{\text{II}}^- = -(p_{\text{II}}^{\text{S}}/p_{\text{II}}^-)_{\alpha \rightarrow 0}$. That is, the divergence of $h_{\text{II}} (\propto \alpha^0)$ is suppressed by an appropriate of $p_{\text{II}} (\propto \alpha^2)$. From now on, we consider this unique solution, which we call the type II solution for brevity.

We next discuss the Znajek condition at the horizon. The condition of eq. (17) can be written in terms of the first-order perturbed functions as

$$kp + \chi^{-1} h = -\frac{a_*}{4\chi}, \quad (55)$$

where $\delta \Phi = h \cos \theta$, $\delta S = 2\lambda \delta F = \lambda p \sin^2 \theta$, $\bar{G} = 1 - \cos \theta$, $\delta G = 0$, and $\omega_{\text{H}} = a_*/(4M)$ are used. This condition is a relation between p and $\chi^{-1} h$, and can be easily incorporated in a type I WKB solution because their magnitudes are of order $p_{\text{I}}^{\pm} \sim \chi^{-1} h_{\text{I}}^{\pm}$. However, the ordering is opposite that of the type II solution, $h_{\text{II}}^{\pm} \sim \chi^{-1} p_{\text{II}}^{\pm}$. The leading-order WKB solutions are not satisfied with the condition (55), so that we have to take into account the higher-order WKB approximation as $p \propto \exp(\chi W) \rightarrow p_{(1)} + \chi^{-1} p_{(2)} + \chi^{-2} p_{(3)} + \dots$, $h \rightarrow h_{(1)} + \chi^{-1} h_{(2)} + \chi^{-2} h_{(3)} + \dots$, where the subscript (n) denotes approximation order n . The condition (55) provides a relation between $p_{(2)}$ and $h_{(1)}$. In the type II solution, we approximate $p_{(1)} = 0$ at the horizon, but have to treat a small correction $\chi^{-1} p_{(2)} (\ll 1)$ in a more elaborate case.

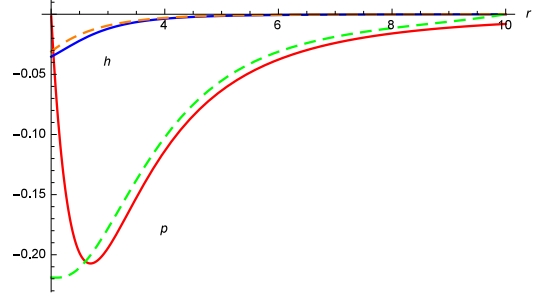


Figure 2. WKB solutions of p and h compared with numerical integration of eqs. (41)–(42). The type II WKB solutions are plotted as solid curves, and the numerical results as dashed ones. The parameters are chosen as $\lambda = 1$, $\chi = 25$ and $a_* = 1$.

3.5 Results

We solve the differential eqs. (41) and (42) with the perturbed Znajek condition of eq. (55) at the horizon and $p = h = h_{,r} = 0$ at outer radius $r/M = 10$. The numerical solution is compared with the type II WKB solution p given by eq. (54) and the corresponding function h by eq. (49). Figure 2 shows good overall agreement except for the boundaries. The agreement in h is better. A minor difference around $r/M = 10$ comes from the choice of outer boundary point; $r/M = 10$ is chosen in the numerical integration, but it is infinity in the WKB solution. There is another difference only in p near the horizon. As discussed in the previous section, the function p_{II} in leading-order WKB approximation goes to zero, but that of the numerical integration goes to a finite value, satisfying the Znajek condition. Our WKB solution represents a piece of a numerical one, which involves another type I WKB solution and higher corrections of χ^{-1} . Note that the Znajek condition (55) leads to $p \approx 0$ at the horizon, if the function h is finite in large χ limit.

A set of differential eqs. (41) and (42) is not so complicated as to prevent integration. However, numerical results cannot be obtained with high precision for large dimensionless parameters because the characteristic lengths become very small. For example, we found that typical upper limits are $\chi < 50$ and $\lambda < 4$. Big or small number is involved in numerical integration like e.g., $\exp(\pm \kappa s) \sim 10^4, 10^{-4}$ even for moderate case $\chi \sim 10$ and $\lambda \sim 1$. Due to this limitation we use the type II leading-order WKB solution in place of numerical integration, and explore the behavior in a much larger χ regime ($\chi \gg 1$) relevant to astrophysical situations. This also provides an advantage of easily analyzing parameter dependence.

Figure 3 shows the electric potential $\delta \Phi = h \cos \theta (\leq 0)$ by the contours. The minimum is located on the polar axis at the horizon ($\theta = 0$, $r/M \rightarrow 2$ or $r_*/M \rightarrow -\infty$), and $\delta \Phi$ increases with either the θ or the r_* coordinate. The figure also shows that $\vec{\nabla} \delta \Phi$ is parallel to $\vec{\nabla} G$ near the horizon; explicitly, $\delta \Phi_{,\theta} = -(h/M) G_{,\theta}$ in the θ direction. Therefore, the function h/M may be regarded as $\delta \Omega_{\text{F}} \equiv -h/M$, the angular velocity of the field line at the horizon. The velocity induced by first-order rotation is in the direction of black hole spin. A typical value of $\delta \Omega_{\text{F}}$ for the model shown in Fig. 2 is $\sim 0.04 a_*/M$. By examining the behavior of h in

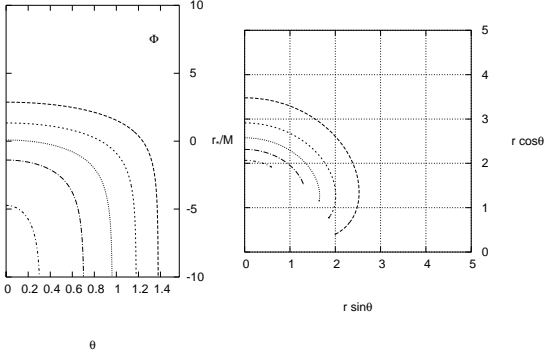


Figure 3. Contour of electric potential $\delta\Phi(\leq 0)$ in the θ - r_* plane (left panel) and at the spherical coordinate (r, θ) (right panel). The minimum of $\delta\Phi$ is located on the polar axis at the horizon ($\theta = 0, r = r_H$).

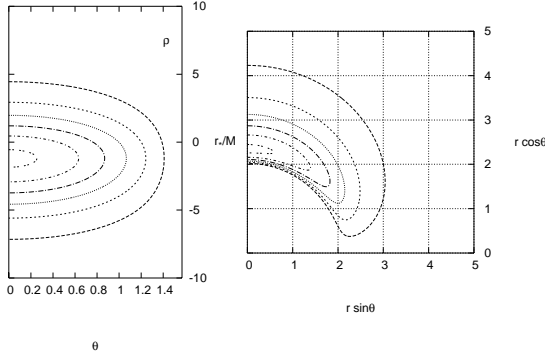


Figure 4. Contour of $\delta n_+/\bar{n}_0 (\propto \delta \rho_e)$ in the θ - r_* plane (left panel) and at the spherical coordinate (r, θ) (right panel). The minimum is located on the polar axis ($\theta = 0, r/M \approx 2.2$).

the WKB solution, we find that the value at the horizon is approximated as $h \approx -a_*/(2^5 \lambda \chi)^{1/2} = -a_*/(2^{5/2} \kappa)$. As the number density (i.e., λ) increases, the deviation from the ideal MHD condition becomes small. Consequently, we have $\delta\Phi \rightarrow 0$ in the large κ limit.

We now consider the density perturbation induced by black hole rotation. Figure 4 shows contours of $\delta n_+/\bar{n}_0 = -\delta n_-/\bar{n}_0 (\propto \delta \rho_e/\bar{n}_0)$ in eq. (40). The minimum, negatively charged region for $a_* > 0$, is located on the polar axis ($\theta = 0$). Unlike $\delta\Phi$, the minimum is not on the horizon, but at $r/M \approx 2.2$. The rate of charge density to the background number density goes to zero towards both radial directions $r_* \rightarrow \pm\infty$ and becomes neutral at the horizon and infinity.

Figure 5 shows the stream function or current flow function $2\delta F = \delta S/\lambda = p \sin^2 \theta$ by contours. Since $\delta F < 0$, both fluids are dragged in the rotational direction of the black hole, that is, $\delta v_\phi^\pm > 0$ (see eq. (38)). The effect is strong on the equator. The contours also show the poloidal current flow δS , where a half loop of current is formed around the minimum ($\theta = \pi/2, r/M \approx 2.5$). In our treatment, we can never impose the condition $\delta S_{,r} = \lambda p_{,r} = 0$ on the equator.

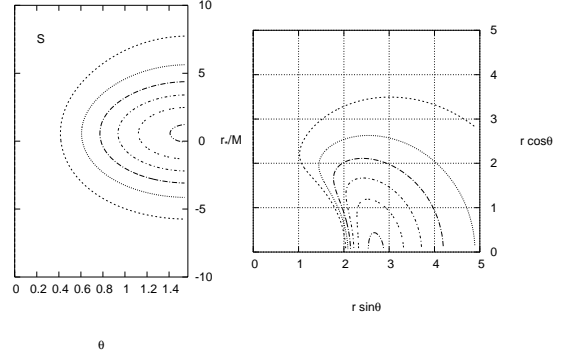


Figure 5. Contour of current function $\delta S/\lambda = 2\delta F(\leq 0)$ in the θ - r_* plane (left panel) and at the spherical coordinate (r, θ) (right panel). The minimum is located on the equator ($\theta = \pi/2, r/M \approx 2.5$).

This means that the poloidal current $j_\theta \propto -p_{,r}$ is allowed to flow into or out from the disk. The function $p_{,r}$ changes sign at $r/M \approx 2.5$. The current emerges up ($j_\theta < 0$) from an outer point, say, $r_2/M > 2.5$, flows along a constant line of δS , and goes down to an inner point $r_1/M < 2.5$ (see eq. (12)). However, there is no potential difference between r_1 and r_2 on the equator. Rather, the origin is attributed to the current sheet on the equator, which produces the radial magnetic field in the vicinity of it. The right panel in (r, θ) coordinates shows a strong concentration of contour lines near the horizon. One might therefore assume a strong surface current on the horizon, but, as discussed in the previous section, the function p in a type II solution goes to zero as $\sim \alpha^2$ toward the horizon, so there is no poloidal surface current on the horizon. The left panel shows that the current vanishes for $r_* \rightarrow -\infty$. At the same time, the toroidal magnetic field $\delta B_\phi \sim \alpha$ also tends to vanish near the horizon.

We calculate the electromagnetic energy power through a sphere of radius r . By integrating the perturbed expression of eq. (16) with respect to θ , we have

$$\delta P_{\text{em}}(r) = \frac{2}{3} \lambda (B_0 M)^2 h p. \quad (56)$$

The power δP_{em} is positive for the type II solution, because $h p > 0$. In other words, outgoing flux is induced. In contrast, the functions for the type I solution in which $h p < 0$ represent incoming energy flux.

Figure 6 shows the outgoing power δP_{em} as a function of r for four models. The function increases with the decrease of r and has a maximum around $r/M = 2.5$, where the longitudinal electric fields and toroidal magnetic fields are significantly produced. However, the power declines toward the horizon and tends to zero owing to $p \rightarrow 0$. This energy flow is therefore produced by the black hole rotation, but is not related to the outgoing flux from the horizon. From numerical calculations, we found that δP_{em} weakly depends on two parameters, (λ, χ) or $(\kappa^2 = \lambda \chi, k = \lambda/\chi)$.

Figure 6 shows that the peak slightly depends on k and increases with k^{-1} , but does not depend on κ . The mathematical reason may be explained as follows: The WKB

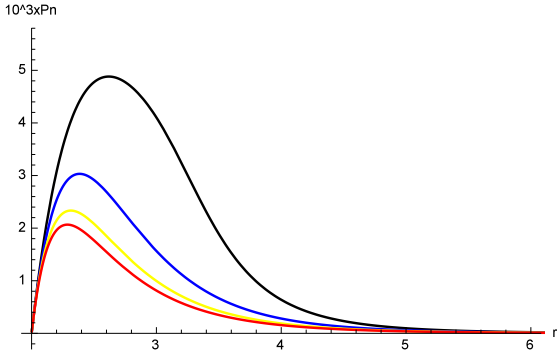


Figure 6. Outgoing electromagnetic power $10^3 \delta P_{\text{em}} / (a_* B_0 M)^2$ as a function of r/M . Four models are shown with $k = 0.025, 0.04, 0.1$ and 1 from top to bottom.

expressions eqs. (49) and (53) yield $p \sim k^{-1/2}$ and $h \sim \chi^{-1} k^{-1/2}$, so their product $\delta P_{\text{em}} \sim \lambda \times k^{-1/2} \times \chi^{-1} k^{-1/2} \sim k^0$ in eq. (56), weakly depends on these parameters, despite p and h strongly depending on them in a different manner. The electromagnetic fields perturbations are approximated as $\delta B_\phi \sim \kappa a_* B_0$ and $\delta \Phi \sim \kappa^{-1} a_* B_0$, but the Poynting power, their product, is almost independent of the parameter κ in the microscopic level.

A typical value is of order $\delta P_{\text{em}} \sim 5 \times 10^{-3} (a_* B_0 M)^2 = 8 \times 10^{-2} (a_* B_n M)^2$, where the magnetic field strength $B_n = B_0/4$ on the horizon is used. Compare this number with the original estimate P_{BZ} by Blandford–Znajek, calculated with the ideal MHD and force-free approximations for a split monopole in the slow rotation limit. The result depends on the undetermined angular velocity Ω_F of the magnetic field lines. With the optimistic choice $\Omega_F = \omega_H/2$, we have $P_{\text{BZ}} = (a_* B_n M)^2/6 \sim 1.6 \times 10^{-1} (a_* B_n M)^2$ in eq. (18). We therefore have $\delta P_{\text{em}} \sim 0.5 P_{\text{BZ}}$. These are of roughly the same order due to the ambiguity of Ω_F involved in P_{BZ} . Finally, we calculate the conversion efficiency, which is a ratio of the electromagnetic power to that of the background inflows given by eq. (37):

$$\frac{\delta P_{\text{em}}}{|P_0|} \sim 2 \times 10^{-3} k^{-1} a_*^2. \quad (57)$$

The efficiency increases with k^{-1} , and reaches $\sim 0.1 a_*^2$ for $k \approx k_c = 2.3 \times 10^{-2}$. This mechanism is efficient in strongly magnetized flow with less abundant matter, that is, smaller k . Contrarily, the conversion becomes less active in high density cases, and may not work for $k > 1$.

4 CONCLUSION

We have explored the electromagnetic structure relevant to outgoing energy flux in a black hole magnetosphere. Our treatment was based on a two-fluid description in which the ideal MHD condition is no longer assumed. By this formalism, we for the first time demonstrated how a longitudinal electric field is produced, even if it vanishes at the outer boundary. We first presented a general framework to construct a stationary axially symmetric structure of the electromagnetic fields and pair plasma flow. The formalism is an extension of our previous work (Kojima & Oogi 2009) for pulsar magnetospheres to a curved spacetime.

For a definite result, we limited discussion to a slowly rotating Kerr black hole and used the perturbation method with respect to the spin parameter. We investigated how and where longitudinal electric fields and toroidal magnetic fields arise in the presence of black hole spin, although both fields are exactly zero in a spherical symmetric monopole model. To study the behavior at macroscopic lengths much larger than the plasma scales, we used a WKB method. By taking into account the first-order rotation, we found a unique solution that describes zero fields at infinity and finite longitudinal electric potential at the horizon. This solution provides outgoing energy power, with magnitude on the same order as that of the original work of Blandford & Znajek (1977).

In comparison with that work, we see a different physics involved in the plasma model. Split monopole magnetic fields as the lowest approximation and perturbations were used in both works. In both, the outgoing power originates from the black hole spin, but the origin is not the same. The black hole horizon, which is causally disconnected to the exteriors, plays a minor role; the energy power generated in our model is damped toward the horizon. The ergoregion is often considered as the origin of longitudinal electric fields and the outgoing power (e.g., Komissarov 2004a; Toma & Takahara 2014). The relation to the existence of the ergoregion is unclear within this work because we can not treat it: The outer ergoregion radius coincides with the horizon, $2M$ in our lowest approximation of the spin. As discussed in Section 2, the ideal MHD condition should be inevitably violated inside the ergoregion for a purely poloidal magnetic field, but this argument may be too strong. The breakdown position is shifted outwardly in our pair model. Finally, Beskin & Kuznetsova (2000) discussed the importance of the pair creation surface in determining the global MHD magnetosphere. The radius in a slowly rotating split-monopole magnetosphere is $\sim 2.52M$. Inflows and outflows are modeled as the boundary of both sides. In our model, the maxima of $|\delta \rho_e|$, $|\delta B_\phi|$, and the luminosity peak are located around $r \sim 2.2\text{--}2.5M$. The pairs are assumed to exist outside the black hole, and to fall into the horizon in the background mean flows. We cannot treat outflows. It is important to study the plasma behavior in the vicinity of the black hole horizon or ergosurface, which leads to outgoing power by the dragging. The crucial radius for the energy conversion is further pushed out by taking into account a realistic two-fluid. Present result was derived under simplified conditions such as steady state, split monopole, certain parameter ranges, boundary conditions and a leading-order WKB approximation. It is true that further study is needed to confirm outgoing Poynting power generation by carefully examining each assumption.

ACKNOWLEDGEMENTS

I am grateful to Kenji Toma and Katuma Kamitamari for useful discussions. This work was supported in part by a Grant-in-Aid for Scientific Research (No. 26400276) from the Japanese Ministry of Education, Culture, Sports, Science and Technology.

REFERENCES

- Bender C. M., Orszag S. A., 1999, Advanced mathematical methods for scientists and engineers I: asymptotic methods and perturbation theory.
- Beskin V. S., 2010, *Physics Uspekhi*, **53**, 1199
- Beskin V. S., Kuznetsova I. V., 2000, *Nuovo Cimento B Serie*, **115**, 795
- Beskin V. S., Par'ev V. I., 1993, *Physics Uspekhi*, **36**, 529
- Blandford R. D., Znajek R. L., 1977, *MNRAS*, **179**, 433
- Contopoulos I., Kazanas D., Papadopoulos D. B., 2013, *ApJ*, **765**, 113
- Khanna R., 1998, *MNRAS*, **294**, 673
- Koide S., Shibata K., Kudoh T., Meier D. L., 2002, *Science*, **295**, 1688
- Kojima Y., Oogi J., 2009, *MNRAS*, **398**, 271
- Komissarov S. S., 2004a, *MNRAS*, **350**, 427
- Komissarov S. S., 2004b, *MNRAS*, **350**, 1431
- Komissarov S. S., 2005, *MNRAS*, **359**, 801
- Komissarov S. S., Barkov M. V., 2009, *MNRAS*, **397**, 1153
- McKinney J. C., 2006, *MNRAS*, **368**, 1561
- McKinney J. C., Tchekhovskoy A., Blandford R. D., 2012, *MNRAS*, **423**, 3083
- Michel F. C., 1973, *ApJ*, **180**, L133
- Nathanail A., Contopoulos I., 2014, *ApJ*, **788**, 186
- Nitta S.-Y., Takahashi M., Tomimatsu A., 1991, *Phys. Rev. D*, **44**, 2295
- Okamoto I., 2012, *PASJ*, **64**, 50
- Okamoto I., 2015, *PASJ*,
- Pan Z., Yu C., 2015, *Phys. Rev. D*, **91**, 064067
- Petrova S. A., 2015, *MNRAS*, **446**, 2243
- Punsly B., ed. 2008, *Black Hole Gravitohydromagnetics Astrophysics and Space Science Library Vol. 355*
- Punsly B., Coroniti F. V., 1990, *ApJ*, **350**, 518
- Spitzer L., 1962, *Physics of Fully Ionized Gases*
- Takahashi M., Nitta S., Tatematsu Y., Tomimatsu A., 1990, *ApJ*, **363**, 206
- Tanabe K., Nagataki S., 2008, *Phys. Rev. D*, **78**, 024004
- Thorne K. S., Price R. H., MacDonald D. A., 1986, *Black holes: The membrane paradigm*
- Toma K., Takahara F., 2014, *MNRAS*, **442**, 2855
- Uzdensky D. A., 2004, *ApJ*, **603**, 652
- Uzdensky D. A., 2005, *ApJ*, **620**, 889
- Znajek R. L., 1978, *MNRAS*, **185**, 833
- van Putten M. H. P. M., Levinson A., 2003, *ApJ*, **584**, 937

APPENDIX A: ENERGY POWER

In this appendix, we consider stationary energy flow. The energy momentum tensor $T^{\mu\nu}$ is a sum of electromagnetic ($T_{\text{em}}^{\mu\nu}$) and matter ($T_{(\pm)}^{\mu\nu}$) parts. The outgoing energy per unit time through a constant radius r is obtained by integrating the energy conservation equation $(\sqrt{-g}T_t^\mu)_{,\mu}/\sqrt{-g} = 0$. The power consists of a sum of the electromagnetic and matter parts:

$$P_{\text{em}}(r) + P_{(+)}(r) + P_{(-)}(r) = - \int (\sqrt{-g}T_t^r) d\theta d\phi. \quad (\text{A1})$$

This total power is independent of r , but each part $P_{\text{em}}, P_{(\pm)}$ in general depends on r because of their interaction. The electromagnetic part P_{em} , that is, the outgoing Poynting flux, can be written as

$$P_{\text{em}}(r) = - \int (\sqrt{-g}T_{\text{em } t}^r) d\theta d\phi = - \frac{1}{2} \int (\Phi_{,\theta} S) d\theta, \quad (\text{A2})$$

where the energy momentum tensor is expressed by electromagnetic fields measured by a ZAMO, $T_{\text{em } t}^r = -\Delta^{1/2}\rho^{-1}(\alpha E^{\hat{\theta}} - \omega\varpi B^{\hat{r}})B^{\hat{\phi}}/4\pi$.

We next consider the plasma energy flow. Power in the $+r$ direction is given for positively or negatively charged fluid components by

$$\begin{aligned} P_{(\pm)}(r) &= - \int (\sqrt{-g}T_{(\pm) t}^r) d\theta d\phi \\ &= 2\pi \int (mK_{\pm} \mp e\Phi) F_{\pm,\theta} d\theta, \end{aligned} \quad (\text{A3})$$

where $T_{(\pm) t}^r = [mn\gamma v^r(1 + \omega\varpi v_{\phi}/\alpha)]_{\pm}$ and Bernoulli integrals K_{\pm} (28) are used.

The total power eq. (A1), a sum of eqs. (A2) and (A3), is expressed as

$$P_{\text{em}} + P_{(+)} + P_{(-)} = -\frac{1}{2} [\Phi S]_{\theta_a}^{\theta_b} + 2\pi m \sum_{\pm} \int_{r=\text{const}} K_{\pm} dF_{\pm}, \quad (\text{A4})$$

where we integrated by parts and used the relation $S = 4\pi e(F_+ - F_-)$. The first term on the right-hand side in eq. (A4) denotes the difference between the two boundary values with respect to θ , and is zero in appropriate cases, e.g., $S(0) = \Phi(\pi/2) = 0$. The second term on the right-hand side is constant with respect to r , unless the plasma flows go out through boundaries θ_a or θ_b . We have thus confirmed that total energy flow is constant in a system consisting of an electromagnetic field and plasma. We consider the right-hand side in eq. (A4) for the linearized perturbations considered in section 3. The first term is also zero up to the second order, since the boundary value of $\delta\Phi S + \Phi\delta S + \delta\Phi\delta S$ becomes zero at $\theta = 0, \pi/2$. We assumed that $K_{\pm} = 1$. and $\delta F_+ = -\delta F_-$, so that the sum in the second term becomes zero.